matters

Older but not slower: ageing does not alter axonal transport dynamics of signalling endosomes *in vivo*

James N Sleigh, Giampietro Schiavo

Sobell Department of Motor Neuroscience and Movement Disorders, Institute of Neurology, University College London

Correspondence
j.sleigh@ucl.ac.uk
giampietro.schiavo@ucl.ac.uk

Disciplines
Neuroscience

Keywords
Aging
Axonal Transport
Neurodegeneration
Peripheral Nerves
Tetanus Toxin

Type of Observation
Standalone

Type of Link
Standard Data

Submitted May 19, 2016
Published Jun 6, 2016

Triple Blind Peer Review
The handling editor, the reviewers, and the authors are all blinded during the review process.

Full Open Access
Supported by the Velux Foundation, the University of Zurich, and the EPFL School of Life Sciences.

Abstract

Efficient bi-directional axonal transport is critical for the function and survival of neurons. Defects in this process have been identified in early stages of several late-onset neurological disease models. Axonal transport is also thought to naturally decline with age, which could exacerbate pathological deficiencies and may alter disease onset and/or progression. Here, by using the atoxic binding fragment of tetanus neurotoxin (HcT), we monitored the transport kinetics of axonal signalling endosomes, which are intracellular compartments essential for neuronal differentiation and homeostasis. HcT can be injected into muscles, where it is taken up by nerve termini and hijacks the retrograde delivery of signalling endosomes. Assessing the dynamic properties of signalling endosomes in live, female, wild-type mice aged from one to over 13 months, we saw no significant alterations in transport speeds or pausing. Our work indicates that decline in signalling endosome kinetics does not occur before one year *in vivo*, suggesting that its deterioration during normal ageing is unlikely to be affecting previously reported disease-associated endosome transport deficits.

Introduction

Neurons possess long, thin processes called axons, which require specialised transport mechanisms for the anterograde (cell soma to axon terminal) and retrograde (terminal to soma) delivery of different cargoes, such as organelles and proteins, to support neuronal function and survival [1]. Defective axonal transport is thought to underlie several neurological conditions, including amyotrophic lateral sclerosis and Alzheimer's disease, as its impairment is amongst the earliest indicators of pathology in disease models [2]. Axonal transport has also been reported to decline with age in a number of different experimental settings including mouse sciatic nerve and hippocampal explants [3] [4], *Drosophila melanogaster* wing preparations [5], and non-invasive, tracer experiments analysing rodent cargo delivery en masse [6] [7] [8] [9]; however, there is little evidence on how ageing affects the real-time transport of individual cargoes in living mammals. We therefore analysed signalling endosome kinetics in peripheral axons of wild-type mice aged one month to over a year by injecting HcT into the muscles of the lower leg with subsequent exposure and imaging of the sciatic nerve (Fig. 1A and Suppl. Video 1).

Objective

Using real-time, intravital imaging, our principal aim was to determine whether wild-type animals show an aging-related decline in axonal transport of signalling endosomes *in vivo* over an extended period.

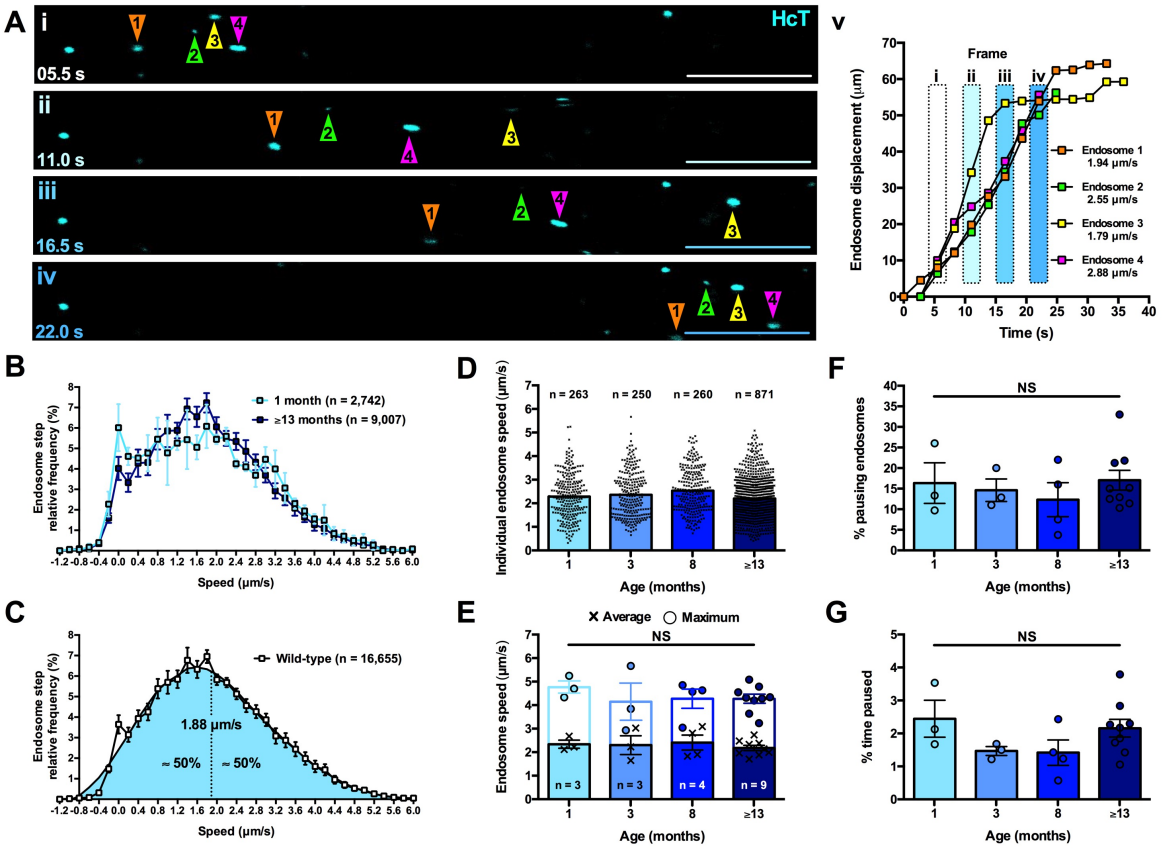

a

Figure Legend

Figure 1. *In vivo* signalling endosome axonal transport dynamics are unchanged up to over a year in wild-type mice.

(A) Representative series of images (i to iv) acquired by time-lapse confocal microscopy of HcT-555 (pseudocoloured cyan) being retrogradely transported (left to right) in sciatic nerve axons from a live wild-type mouse (postnatal day 408). Four individual endosomes are tracked by coloured triangles (iv), the displacement profiles of which have been plotted (v). Scale bars = 10 µm.

(B) The speed distribution curves of signalling endosome are similar for 1 month and ≥13 month old wild-type animals. The same holds true for the 3 and 8 month data, which are not plotted.

(C) Speed distribution curve produced by combining data from 4 different time points (1, 3, 8 and ≥13 months; 19 mice). A smoothened curve is fitted to the data, which shows that approximately 50% of individual endosome steps are faster than 1.88 µm/s. A value of 1.89 µm/s was calculated from the raw data.

(D) The mean average speed of individual signalling endosomes across the four ages are plotted. Each data point represents an individual endosome.

(E) There is no significant difference between ages in the mean average (×, P =0.851, one-way ANOVA) and the maximum (O, P =0.757, one-way ANOVA) signalling endosome speeds calculated individually for each mouse.

(F-G) No difference is also detected between ages in the percentage of endosomes pausing for at least one frame (F, P =0.876, one-way ANOVA) or the percentage of time paused (G, P =0.221, one-way ANOVA). Pairwise statistical comparisons of the data from different ages in panels E-G were also not significant (P >0.05, Tukey's multiple comparisons test). NS, not significant. Means ± standard error of the mean (S.E.M.) are plotted for all graphs. n =3 (1 month), 3 (2 months), 4 (8 months), and 9 (≥13 month).

Supplementary Video 1. *In vivo* imaging of axonal transport.

Representative video constructed from images acquired by time-lapse confocal microscopy of HcT-555 (pseudocoloured cyan) being retrogradely transported (left to right) in exposed sciatic nerve axons of a live, anaesthetised, wild-type mouse (P408). HcT was injected into the gastrocnemius and tibialis anterior muscles of the right leg, and is being transported towards the spinal cord. The video consists of 199 frames, covering 546 s, and is being played at a rate of 5 frames/s. The video is 66.4 mm × 18.6 mm.

Animals

Wild-type mice were maintained as breeding trios on a predominantly C57BL/6 background. Only female mice were analysed. Animals used for the 1, 3, 8, and ≥13 month time points were 30–31 (mean =30.3), 90–93 (mean =91.7), 251–253 (mean =251.5), and 393–426 (mean =401.1) days old, respectively.

Injection and imaging of fluorescently labelled HcT

To image the *in vivo* kinetics of signalling endosomes labelled with HcT, the detailed protocol of Gibbs *et al.* 2016 was closely followed [15]. Briefly, HcT (HcT441, residues 875-1315), fused at its amino terminal to an improved cysteine-rich tag [16] and a human influenza haemagglutinin epitope, was expressed, purified and fluorescently labelled with AlexaFluor555 C2 maleimide (Life Technologies, A-20346). On the day of imaging, under surgical conditions mice were anaesthetised using isofluorane (National Veterinary Services, UK) and the gastrocnemius and tibialis anterior muscles of the right leg exposed by two small incisions. Each muscle was injected with approximately 5–7 µg of HcT pre-mixed with 25 ng recombinant human BDNF (Peprotech, 450-02) to aid uptake of the toxin. 4–6 h later, the right sciatic nerve was carefully exposed at the mid-thigh level in anaesthetised mice, which were subsequently transferred to the stage of an inverted LSM 780 laser scanning microscope (Zeiss) within an environmental chamber pre-warmed and set to 37°C. The sciatic nerve was then located using a 63x Plan-Apochromat oil immersion objective lens (Zeiss), and an area containing labelled axons selected and imaged at 100x digital zoom. At least three axons were imaged per animal within one hour of first being anaesthetised. 1–4 animals were imaged in 1 day, and frames were acquired every 2.4–3.3 s. Image series were converted into AVI files and signalling endosome speeds assessed using Kinetic Imaging Software to measure endosome distance covered between two consecutive frames. Endosomes were included in the analysis if they could be tracked for at least five consecutive frames, and did not pause for more than ten consecutive images. We estimate that fewer than one endosome per animal fell into this latter category. An average of 87 endosomes per animal was tracked.

Statistical analysis

Data were assumed to be normally distributed unless evidence to the contrary could be provided by the D'Agostino and Pearson omnibus normality test. Normally distributed data were statistically analysed using a one-way analysis of variance (ANOVA) with Tukey's multiple comparisons tests or a two-way ANOVA. GraphPad Prism 6 software was used for all statistical analyses and figure production.

Results & Discussion

HcT was injected into the gastrocnemius and tibialis anterior muscles of the right hind limb of live, anaesthetised, wild-type, female mice at four different ages of 1, 3, 8, and ≥13 months. 4–6 h post-injection, the right sciatic nerve was exposed and imaged using time-lapse confocal microscopy in order to identify and track individual HcT-containing signalling endosomes being retrogradely transported towards the spinal cord (Fig. 1A and Suppl. Video 1). The speed of all individual endosome steps between two consecutive frames was calculated and relative frequencies plotted (Fig. 1B-C). The speed distribution curves of all four time points were very similar (Fig. 1B, only 1 and ≥13 month data are shown). We therefore combined the data from all ages into one curve in order to produce a reference speed profile for wild-type mice (Fig. 1C). The average speed of single endosomes across at least five consecutive frames was also plotted for the four time points (Fig. 1D). When these values were averaged to produce mean and maximum endosome speeds for each animal, we saw no significant differences between any of the time points (Fig. 1E, average speed, P =0.851, one-way ANOVA; maximum speed, P =0.757, one-way ANOVA; pairwise comparisons, P >0.05, Tukey's multiple

comparisons test). Moreover, there was no difference in either the percentage of endosomes pausing for at least one frame or the percentage of time spent paused (Fig. 1F-G, P =0.876, one-way ANOVA; maximum speed, P =0.221, one-way ANOVA; pairwise comparisons, P >0.05, Tukey's multiple comparisons test).

Several studies have provided indirect evidence that axonal transport declines with age by using non-invasive approaches. For example, radiolabelled tracers have been used to show that slow axonal transport is compromised by 24 months in rat ventral motor axons and optic nerves [8], while α-synuclein transport velocity is reduced by 11 months in mouse sciatic nerves [7]. Similarly, magnetic resonance imaging has shown that axonal transport rates are diminished by 13 months in rat brains, and are in decline in the mouse olfactory bulb by 15 months [6]. Nevertheless, these studies may be affected by axon loss, and do not directly assess axonal transport of individual cargoes in identifiable axons in live animals. Only a single previous report has used intravital imaging to assess the transport of individual cargoes in living, anaesthetised mice. Takihara *et al.* reported that the duration, distance and speed of mitochondrial transport in retinal ganglion neurons increased from 2 to 4 months of age, but then declined by 12–13 months, getting worse by 23–25 months [10]. Our data presented here contrast with these findings up to 13 months and indicate that axonal transport of signalling endosomes remains unchanged *in vivo* in wild-type mice aged over a year. This discrepancy may be caused by differences in myelination, which is known to affect the stability of the microtubules used by molecular motors for axonal transport [11]. Alternatively, it may reflect the type of cargo being transported [12], or innate properties of the central and peripheral nervous systems [4].

Conclusions

Wild-type, female mice show no difference in the axonal transport dynamics of signalling endosomes in the peripheral nervous system between four time points spanning one month to over a year. This work is the first to show that real-time axonal transport speeds and pausing are unaffected in live, anaesthetised mice aged above a year. These data indicate that previously reported defects in endosome dynamics in mouse models of late-onset nervous system disease using fluorescently labelled HcT [12] are unlikely to be compounded by natural, age-related decline in the transport process, thus also facilitating the future analysis of slower progressing disease models.

Limitations

The presented analyses only include data from female mice, which may not be reflective of both sexes. We have generated data from males at 1 and 3 months, and there does not appear to be a difference between sexes (n =3; average speed, P =0.972; maximum speed, P =0.801; % pausing endosomes, P =0.550; % time paused, P =0.304; two-way ANOVA, data not shown). Moreover, males and females have previously been reported to show no distinctions in vesicular and mitochondrial transport dynamics in nerve explant preparations across multiple ages [4]; however, although unlikely, this may not be true *in vivo* for signalling endosomes at the later time points of 8 and ≥13 months. Moreover, we only analysed a single type of cargo, which move exclusively in the retrograde direction. In addition, transport kinetics are not evaluated beyond 13 months of age, and hence we cannot comment on what happens towards the end of the natural lifespan of laboratory mice. When injected into muscle, HcT is taken up at both neuromuscular junctions (NMJs, motor termini) and muscle spindles (proprioceptive sensory termini). The sciatic nerve consists of both motor and sensory axons, so we cannot be certain about the type of neuron analysed for each animal using this modality of injection. Nevertheless, given that muscles possess considerably more NMJs than spindles (for example, approximately 20 fold more in the cleidomastoid muscle [13] [14]) and approximately 80% of HcT-containing sciatic axons stain for the motor marker ChAT [12], it is likely that we were predominantly analysing motor nerves. Finally, due to variability in the amount of HcT uptake between different nerves, we cannot reliably measure the frequency of cargoes being transported as has been done previously [3] [4]. It would be important to grow mice to 2 years and see whether the previously reported

transport deficits in neuronal explants at this age [4] are observed in an *in vivo* setting. Furthermore, intravital imaging of other axonal, bi-directionally transported cargoes such as mitochondria would allow us to determine whether anterograde transport is disturbed and whether these findings are cargo specific, central or peripheral nervous system dependent, or generally applicable.

Additional Information

Methods

Animals

Wild-type mice were maintained as breeding trios on a predominantly C57BL/6 background. Only female mice were analysed. Animals used for the 1, 3, 8, and ≥13 month time points were 30–31 (mean =30.3), 90–93 (mean =91.7), 251–253 (mean =251.5), and 393–426 (mean =401.1) days old, respectively.

Injection and imaging of fluorescently labelled HcT

To image the *in vivo* kinetics of signalling endosomes labelled with HcT, the detailed protocol of Gibbs *et al.* 2016 was closely followed [15]. Briefly, HcT (HcT441, residues 875-1315), fused at its amino terminal to an improved cysteine-rich tag [16] and a human influenza haemagglutinin epitope, was expressed, purified and fluorescently labelled with AlexaFluor555 C2 maleimide (Life Technologies, A-20346). On the day of imaging, under surgical conditions mice were anaesthetised using isofluorane (National Veterinary Services, UK) and the gastrocnemius and tibialis anterior muscles of the right leg exposed by two small incisions. Each muscle was injected with approximately 5–7 µg of HcT pre-mixed with 25 ng recombinant human BDNF (Peprotech, 450-02) to aid uptake of the toxin. 4–6 h later, the right sciatic nerve was carefully exposed at the mid-thigh level in anaesthetised mice, which were subsequently transferred to the stage of an inverted LSM 780 laser scanning microscope (Zeiss) within an environmental chamber pre-warmed and set to 37°C. The sciatic nerve was then located using a 63x Plan-Apochromat oil immersion objective lens (Zeiss), and an area containing labelled axons selected and imaged at 100x digital zoom. At least three axons were imaged per animal within one hour of first being anaesthetised. 1–4 animals were imaged in 1 day, and frames were acquired every 2.4–3.3 s. Image series were converted into AVI files and signalling endosome speeds assessed using Kinetic Imaging Software to measure endosome distance covered between two consecutive frames. Endosomes were included in the analysis if they could be tracked for at least five consecutive frames, and did not pause for more than ten consecutive images. We estimate that fewer than one endosome per animal fell into this latter category. An average of 87 endosomes per animal was tracked.

Statistical analysis

Data were assumed to be normally distributed unless evidence to the contrary could be provided by the D'Agostino and Pearson omnibus normality test. Normally distributed data were statistically analysed using a one-way analysis of variance (ANOVA) with Tukey's multiple comparisons tests or a two-way ANOVA. GraphPad Prism 6 software was used for all statistical analyses and figure production.

Supplementary Material

Please see https://sciencematters.io/articles/201605000018.

Funding Statement

This work was supported by a Wellcome Trust Sir Henry Wellcome Postdoctoral Fellowship (103191/Z/13/Z) [JNS], a Wellcome Trust Senior Investigator Award (107116/Z/15/Z) [GS] and University College London [GS].

Acknowledgements

The authors would like to thank members of the Schiavo and Prof. Linda Greensmith laboratories (Institute of Neurology, UCL) for productive discussions, and Katherine L. Gibbs and Bernadett Kalmar for sharing experimental expertise.

Ethics Statement

All mouse handling and experiments were performed under license from the United Kingdom Home Office in accordance with the Animals (Scientific Procedures) Act (1986) and approved by the University College London - Institute of Neurology Ethics Committee.

Citations

[1] Sandra Maday et al. "Axonal Transport: Cargo-Specific Mechanisms of Motility and Regulation". In: *Neuron* 84.2 (Oct. 2014), pp. 292–309. DOI: 10.1016/j.neuron.2014.10.019. URL: http://dx.doi.org/10.1016/j.neuron.2014.10.019.

[2] Stéphanie Millecamps and Jean-Pierre Julien and. "Axonal transport deficits and neurodegenerative diseases". In: *Nature Reviews Neuroscience* 14.3 (Jan. 2013), pp. 161–176. DOI: 10.1038/nrn3380. URL: http://dx.doi.org/10.1038/nrn3380.

[3] Jonathan Gilley et al. "Age-dependent axonal transport and locomotor changes and tau hypophosphorylation in a "P301L" tau knockin mouse". In: *Neurobiology of Aging* 33.3 (Mar. 2012), 621.e1–621.e15. DOI: 10.1016/j.neurobiolaging.2011.02.014. URL: http://dx.doi.org/10.1016/j.neurobiolaging.2011.02.014.

[4] Stefan Milde et al. "Axonal transport declines with age in two distinct phases separated by a period of relative stability". In: *Neurobiology of Aging* 36.2 (Feb. 2015), pp. 971–981. DOI: 10.1016/j.neurobiolaging.2014.09.018. URL: http://dx.doi.org/10.1016/j.neurobiolaging.2014.09.018.

[5] A. Vagnoni, P. C. Hoffmann, and S. L. Bullock and. "Reducing Lissencephaly-1 levels augments mitochondrial transport and has a protective effect in adult Drosophila neurons". In: *Journal of Cell Science* 129.1 (Nov. 2015), pp. 178–190. DOI: 10.1242/jcs.179184. URL: http://dx.doi.org/10.1242/jcs.179184.

[6] Jieun Kim et al. "Quantitative in vivo measurement of early axonal transport deficits in a triple transgenic mouse model of Alzheimer's disease using manganese-enhanced MRI". In: *NeuroImage* 56.3 (June 2011), pp. 1286–1292. DOI: 10.1016/j.neuroimage.2011.02.039. URL: http://dx.doi.org/10.1016/j.neuroimage.2011.02.039.

[7] Wenxue Li et al. "Axonal transport of human α-synuclein slows with aging but is not affected by familial Parkinson's disease-linked mutations". In: *Journal of Neurochemistry* 88.2 (Dec. 2003), pp. 401–410. DOI: 10.1046/j.1471-4159.2003.02166.x. URL: http://dx.doi.org/10.1046/j.1471-4159.2003.02166.x.

[8] Irvine G. McQuarrie, Scott T. Brady, and Raymond J. Lasek and. "Retardation in the slow axonal transport of cytoskeletal elements during maturation and aging". In: *Neurobiology of Aging* 10.4 (July 1989), pp. 359–365. DOI: 10.1016/0197-4580(89)90049-3. URL: http://dx.doi.org/10.1016/0197-4580(89)90049-3.

[9] Satoshi Minoshima and Donna Cross and. "In vivo imaging of axonal transport using MRI: aging and Alzheimer's disease". In: *European Journal of Nuclear Medicine and Molecular Imaging* 35.S1 (Jan. 2008), pp. 89–92. DOI: 10.1007/s00259-007-0707-8. URL: http://dx.doi.org/10.1007/s00259-007-0707-8.

[10] Yuji Takihara et al. "In vivo imaging of axonal transport of mitochondria in the diseased and aged mammalian CNS". In: *Proceedings of the National Academy of Sciences* 112.33 (Aug. 2015), pp. 10515–10520. DOI: 10.1073/pnas.1509879112. URL: http://dx.doi.org/10.1073/pnas.1509879112.

[11] L. L. Kirkpatrick and S. T. Brady. "Modulation of the axonal microtubule cytoskeleton by myelinating Schwann cells". In: *Journal of Neuroscience* 14 (1994), pp. 7440–7450.

[12] L. G. Bilsland et al. "Deficits in axonal transport precede ALS symptoms in vivo". In: *Proceedings of the National Academy of Sciences* 107.47 (Nov. 2010), pp. 20523–20528. DOI: 10.1073/pnas.1006869107. URL: http://dx.doi.org/10.1073/pnas.1006869107.

[13] Juan C. Tapia et al. "Pervasive Synaptic Branch Removal in the Mammalian Neuromuscular System at Birth". In: *Neuron* 74.5 (June 2012), pp. 816–829. DOI: 10.1016/j.neuron.2012.04.017. URL: http://dx.doi.org/10.1016/j.neuron.2012.04.017.

[14] A. M. Brichta, R. J. Callister, and E. H. Peterson and. "Quantitative analysis of cervical musculature in rats: Histochemical composition and motor pool organization. I. Muscles of the spinal accessory complex". In: *The Journal of Comparative Neurology* 255.3 (Jan. 1987), pp. 351–368. DOI: 10.1002/cne.902550304. URL: http://dx.doi.org/10.1002/cne.902550304.

[15] Katherine L. Gibbs et al. "In vivo imaging of axonal transport in murine motor and sensory neurons". In: *Journal of Neuroscience Methods* 257 (Jan. 2016), pp. 26–33. DOI: 10.1016/j.jneumeth.2015.09.018. URL: http://dx.doi.org/10.1016/j.jneumeth.2015.09.018.

[16] Brent R Martin et al. "Mammalian cell–based optimization of the biarsenical-binding tetracysteine motif for improved fluorescence and affinity". In: *Nature Biotechnology* 23.10 (Sept. 2005), pp. 1308–1314. DOI: 10.1038/nbt1136. URL: http://dx.doi.org/10.1038/nbt1136.